LEFT-HANDED MICROSTRIP LINES WITH MULTIPLE COMPLEMENTARY SPLIT-RING AND SPIRAL RESONATORS

V. Crnojević-Bengin[1], V. Radonić[1], and B. Jokanović[2]

[1] Dept. of Electronics, Faculty of Technical Sciences, University of Novi Sad, Serbia,

[2] Institute Imtel, Belgrade, Serbia

ABSTRACT: *Negative-permeability sub-wavelength particles, namely split-ring resonators and spiral resonators, are compared and their performances analyzed for a different number of concentric rings and spiral turns, respectively. Left-handed lines are designed, fabricated and measured that use multiple complementary split-ring and spiral resonators. More compact structures are obtained, with improved characteristics.*

Key Words: *Left-handed metamaterials; Split-Ring Resonators; Spiral resonators; Bandpass Filters.*

1. INTRODUCTION

Recently, revolutionary results were obtained in the field of metamaterials, artificial structures composed of a number of unit cells with sub-wavelength dimensions that exhibit electromagnetic

properties generally not found in nature. Due to the very small size of the unit cell, quasi-static analysis can be performed and the concept of artificial effective media can be applied. Therefore, metamaterials can be tailored to exhibit arbitrarily small or large, or even negative, values of the effective permittivity and permeability. Double-negative or left-handed (LH) media are those that simultaneously exhibit negative values of effective permittivity and permeability in a certain frequency range.

The behavior of LH media was theoretically analyzed by Russian physics Victor Veselago in the late sixties, [1]. However, the first structure that exhibits negative permittivity by decreasing the plasmon frequency into the microwave range was proposed in the mid nineties, [2]. Shortly afterwards, a particle called split-ring resonator (SRR) was introduced, that provides negative permeability at microwave frequencies, [3]. By superimposing these two structures, the existence of left-handed metamaterials was experimentally proved in 2001, [4].

An array of SRRs exhibits the extreme values of effective magnetic permeability in the vicinity of resonance, namely highly positive/negative in a narrow band below/above the quasi-static resonant frequency of the rings. Although having a narrow frequency range with negative permeability, the configurations using SSRs have driven a lot of attention, [5], [6].

In the microstrip technology, SRRs can only be etched in the upper substrate side, next to the host transmission line. To enhance the coupling, the distance between the line and the rings should be as small as possible. Therefore, square or rectangle geometries are typically used instead of the originally proposed circular ones. A microstrip line loaded with the SRRs is a

single-negative medium, therefore exhibiting a stop-band characteristic. It is well known, [3], that using two concentric rings with slits on the opposite sides, instead of just one, greatly increases the capacitance of the structure (as well as its inductance), and therefore reduces its resonant frequency. In this paper, multiple SRR geometries are investigated, that consist of N concentric rings, instead of just one or two.

Following the first ideas of Pendry, spiral resonators (SR) can also be used as negative-μ sub-wavelength particles. The influence of the number of turns, N, to the performances of the SR is also investigated, and compared to the SRR case.

Using the Babinet principle, complementary split-ring-resonator (CSRR) was proposed in [7]. CSRRs are etched in the ground plane, beneath the microstrip, with their axes parallel to the vector of the electric field, thus contributing to the negative effective permittivity. In order to obtain left-handed behaviour, particles that introduce negative effective permeability must be added to the structure. This is achieved by periodically etching capacitive gaps in the conductor strip. Using the same approach, LH microstrip line with complementary spiral resonators (CSR) and capacitive gaps can be designed.

In this paper, influence of number of concentric rings/spiral turns, N, to performances of the proposed LH microstrip lines is analyzed. I order to compare lines using CSRRs with those using CSRs, the dimensions of CSR are optimized to achieve same resonant frequency as the CSRR. Proposed lines are simulated, fabricated and measured.

2. MICROSTRIP LINES LOADED WITH MULTIPLE SRR AND MULTIPLE SR

In order to investigate the influence of the number of concentric rings, microstrip lines loaded with multiple ($N \geq 2$) square SRRs are first analyzed. To enhance the coupling, separation between the concentric rings, as well as between the outer ring and the microstrip line is chosen to be the minimal achievable in standard PCB technology, i.e. equal to 100 μm. All circuits are realized on a 1.27 mm thick Taconic CER-10 substrate, having $\varepsilon_r = 9.8$ and dielectric loss tangent equal to 0.0025. In order to increase the inductance of the unit cell, lines having minimal line width achievable are used, equal to 100 μm. Microstrip line loaded with SRR comprising of $N=2$ concentric rings is shown in Figure 1.

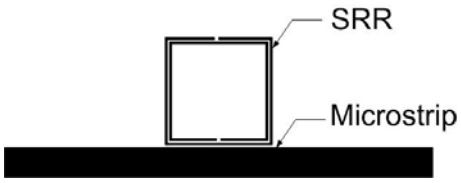

Figure 1 Microstrip line loaded with $N=2$ SRR

Apart from the SRR, microstrip lines loaded with spiral resonators having different number of turns, also denoted with N, are investigated. In Figure 2, multiple SRR and multiple SR geometries are shown for the cases $N=2$ and $N=9$. The outer dimensions of both the SRR and the SR are equal to 5 x 5 mm, i.e. $\lambda/16$ x $\lambda/16$ on a given substrate, while concentric rings and turns are added to the inner sides of the structures. Also, for a given N, both the SRR and the SR have approximately the same line length.

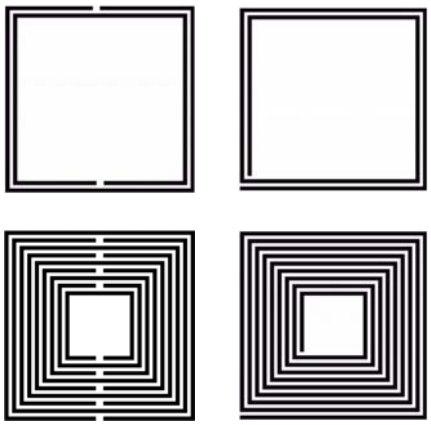

(a) (b)

Figure 2 (a) SRR with *N*=2 (top) and *N*=9 (bottom) concentric rings, (b) SR with *N*=2 (top) and *N*=9 (bottom) turns

Performances of SRR- and SR-loaded microstrip lines were first determined using EMSight, EM simulator in Microwave Office, for the lossless case. Tables 1 and 2 show simulation results for both structures for different *N*, where f_{s1} and f_{s2} denote resonant frequencies of the first and the second stop band, respectively, *R* is the ratio between these two frequencies, s_{21_0} is insertion loss at f_{s1} and *BW* is a 3dB stop-band bandwidth.

TABLE 1 Simulation results for microstrip line loaded with SRR consisting of *N* concentric rings

N	2	3	4	5	6	7	8	9
f_{s1}, GHz	2.34	2.13	2.02	1.97	1.95	1.94	1.94	1.94
f_{s2}, GHz	4.65	3.67	3.33	3.15	3.06	3.02	3	2.99
R	1.984	1.724	1.648	1.596	1.569	1.556	1.549	1.544
$s_{21\ 0}$, dB	-66.4	-75	-72.7	-74.7	-74.3	-75	-74.3	-75
BW, kHz	19	7	6	5	4	3	3	2

TABLE 2 Simulation results for microstrip line loaded with SR consisting of *N* turns

N	2	3	4	5	6	7	8	9
f_{s1}, GHz	1.148	0.785	0.628	0.541	0.489	0.456	0.435	0.422
f_{s2}, GHz	3.42	2.2	1.67	1.38	1.209	1.097	1.205	0.98
R	2.98	2.9	2.803	2.551	2.472	2.405	2.356	2.320
$s_{21\ 0}$, dB	-80.9	-85.9	-93.8	-89.1	-82.2	-78.9	-80.2	-85.3

Bandwidth is not shown in Table 2, since it was bellow 1 kHz, which is the resolution of the EMSight. However, it was possible to notice that, as in the case of the SRR, bandwidth was reduced by increasing number of turns, *N*. By comparing results from Tables 1 and 2, it can be seen that spiral geometries exhibit significantly lower resonant frequencies for the same dimensions of the particles, as well as the higher attenuation levels in the stop-band. In both SRR and SR cases, adding multiple rings significantly reduced resonant frequency, due to the increased inductance and capacitance of the structure. Also, with the increased *N*, second harmonic was shifted towards the lower frequencies, i.e. *R* was reduced.

For both structures, certain saturation can be observed for higher values of *N*. Adding more then 5 concentric rings in the SRR, results in a very small change of the performances: resonant frequency is lowered for less then 1%, while the other parameters also vary very slightly. The same behavior can be observed in the case of the SR with number of turns greater then 7. The explanation of this phenomenon is that the efficiency of excitation of the particle by axial magnetic field deteriorates when its middle section is occupied. For that reason, only multiple geometries with $N<5$ will be investigated in the following section.

3. LEFT-HANDED MICROSTRIP LINES USING MULTIPLE CSRR AND MULTIPLE CSR

Left-handed lines using 100 μm gaps in the microstrip and CSRRs/CSRs with different number of concentric rings/turns, *N*, are analyzed. As an example, the proposed line using *N*=4 CSRRs is shown in Figure 3 where both top (dark grey) and bottom (light grey) conductive layers are shown. The overall dimensions of a single CSRR are equal to 5 x 5 mm, i.e. λ/16 x λ/16 on a given substrate. All lines are realized on a 1.27mm Taconic CER-10 substrate, having ε_r= 9.8 and dielectric loss tangent equal to 0.0025.

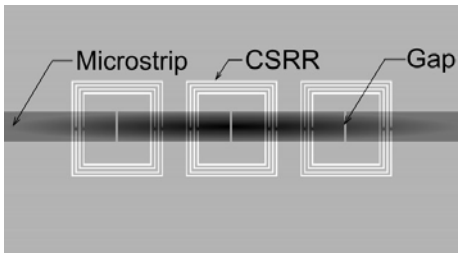

Figure 3 An example of the proposed LH microstrip line, using *N*=4 CSRRs

Left-handedness of proposed structures is evident from the comparison of the phases of transmission coefficients obtained for a different number of unit cells *M*, for LH line using *N*=2 CSRRs, Figure 4. It can be seen that a phase advance exists in the passband, thus demonstrating backward propagation.

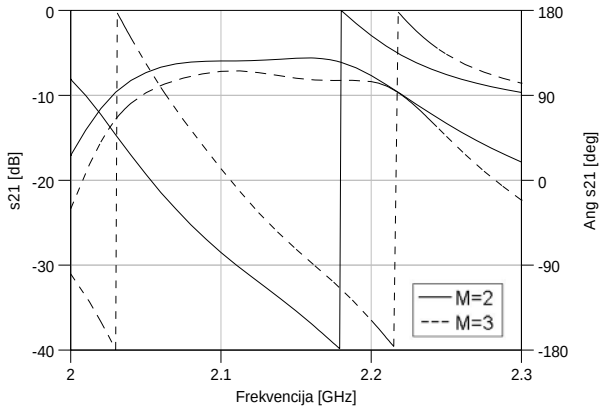

Figure 4 Transmission coefficient and phase propagation for the LH microstrip lines using *N*=2 CSRRs with *M*=2 and *M*=3 unit cells

The simulations results for the LH microstrip line using multiple CSRRs are compared in Table 3 for a different number of concentric rings, *N*. Proposed lines can be characterized in terms of band pass filters, where f_{c1} and f_{c2} denote central frequencies of the first and second harmonic, *R* is the ratio between these two frequencies, s_{21_0} is insertions loss in the first pass band, *BW* is a 3 dB bandwidth, Q_L is loaded and Q_U is unloaded quality factor.

TABLE 3 Simulation results for the proposed LH microstrip line using multiple CSRRs with *N* concentric rings

N	2	3	4
f_{c1}, GHz	2.123	1.913	1.797
f_{c2}, GHz	4.92	5.32	5.8
R	2.32	2.78	3.23
$s_{21\ 0}$, dB	-5.6	-6.39	-6.73
BW, MHz	185	173.05	170.8
Q_L	11.47	11.06	10.52
Q_U	15.83	14.37	13.36

The simulations results for the LH microstrip line using multiple CSRs are presented in Table 4 and compared in Figure 5 for a different number of turns, *N*.

TABLE 4 Simulation results for the proposed LH microstrip line using multiple CSRs with *N* turns

N	2	3	4
f_{c1}, GHz	1.059	0.7179	0.560
f_{c2}, GHz	5.41	5.54	5.63
R	5.11	7.72	10.04
$s_{21\ 0}$, dB	-10.4	-11.1	-11
BW, MHz	91.2	66.3	45
Q_L	11.61	10.82	12.46
Q_U	12.78	11.73	13.54

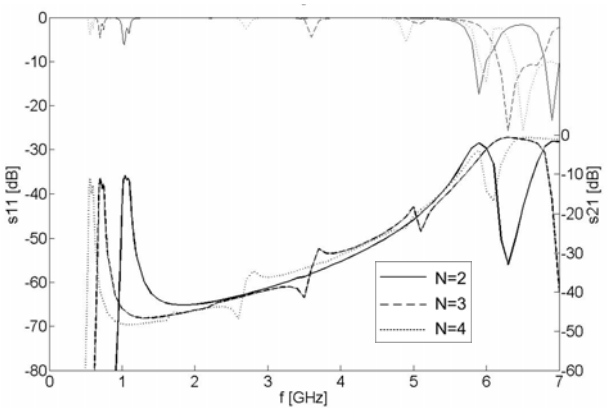

Figure 5 Comparison of the simulated responses of the proposed LH line using CSRs with different number of turns, *N*

In both the CSRR and the CSR case, a significant reduction of resonant frequency is achieved by increasing *N*, due to the increased inductance and capacitance of the structures. The second

harmonic is significantly shifted towards the higher frequencies, i.e. ratio R is increased, therefore resulting in wide and deep stop-bands. The LH line using CSRs exhibits more narrow pass bands then its CSRR counterpart, but with higher insertion loss. Figure 5 reveals that, unlike the CSRR, LH line using CSRs exhibits sharp transitions on both sides of the pass band.

The insertion loss increases with N in both cases, which can be explained by two mechanisms. Firstly, line-length of the particle increases significantly with N, thus contributing to losses. Secondly, adding more concentric rings/turns reduces the metallic area in the middle section of the particle, exposed to the axial electric field, therefore deteriorating excitation and resulting in poorer coupling to the microstrip. This also explains the decrease of the quality factors observed for the increasing N.

In order to fully compare LH lines using CSRRs and CSRs, dimensions of the N=2 CSRs are optimized to achieve the same resonant frequency as N=2 CSRRs. The line width and spacing are fixed and equal to 100 μm, while the outer dimensions of the CSR were varied. In that way, CSR with dimensions 2.9 mm x 2.9 mm was obtained, thus achieving reduction of over 66% in the particle's area, for a given central frequency. Comparison of the simulation results is presented in Table 5 for the lossy case.

It can be seen that, due to its shape, the line using CSRs exhibits much higher insertion loss, as well as the narrower bandwidth. Attenuation in the stop-band is approximately equal for both lines.

TABLE 5 Simulation results for LH microstrip line using *N*=2 CSRRs and *N*=2 CSRs with optimized dimensions

	CSR	CSRR
Dimensions, mm	2.9 x 2.9	5 x 5
f_{c1}, GHz	2.012	2.122
f_{c2}, GHz	7.2	4.99
R	3.59	2.35
$s_{21\ 0}$, dB	-13.3	-5.6
BW, MHz	61.15	185
Q_L	32.90	11.47
Q_U	34.51	15.83

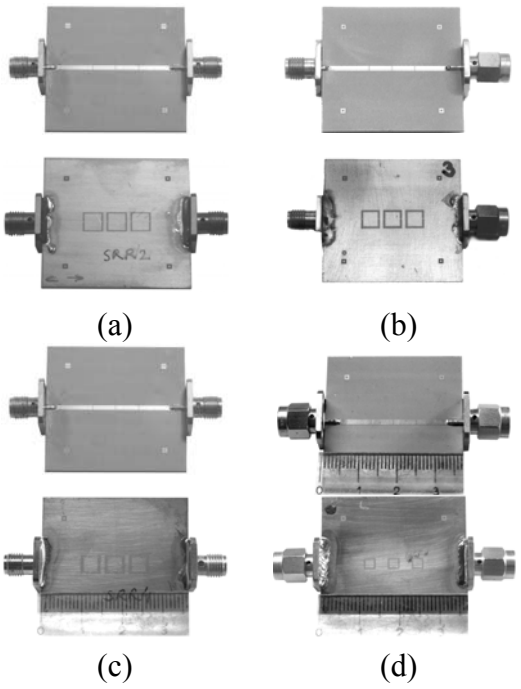

Figure 6 Top (upper) and bottom (lower) sides of fabricated structures: LH line using (a) *N*=2 CSRRs, (b) *N*=3 CSRRs, (c) *N*=4 CSRRs, (d) *N*=2 CSRs with optimized dimensions.

4. MEASUREMENT RESULTS

To validate simulation results, LH microstrip lines using CSRRs with two, three and four concentric rings, and 2.9 x 2.9 mm N=2 CSRs were fabricated in standard PCB technology. Photographs of the top and bottom layers of all fabricated structures are shown in Figure 6.

The simulation and measurement results of the LH line using multiple CSRRs are compared in Figure 7, for different values of N.

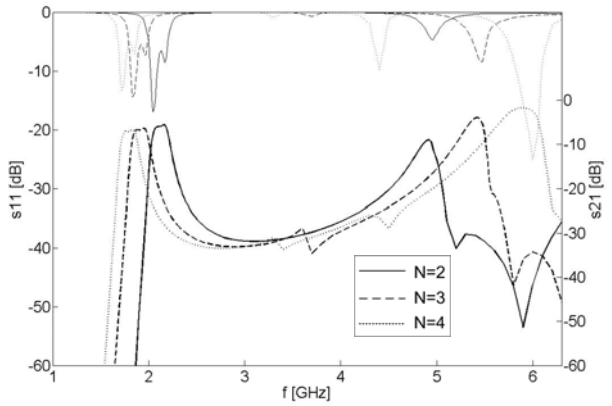

(a)

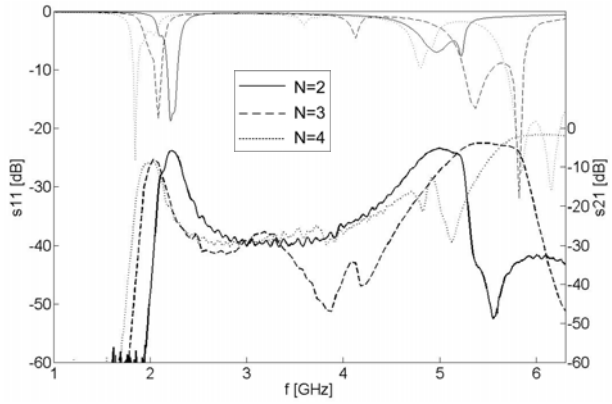

(b)

Figure 7 (a) Simulation and (b) measurement results for LH lines using multiple CSRRs

A good agreement between simulated and measured values can be observed, except for a shift in frequency approximately equal to 5% that occurred in all cases. Since manufacturer specifications for substrate material allow εr variations in the range +/- 0.5 as well as variations of the substrate thickness, the disagreement can be explained by the discrepancy between the actual and the simulated values of the dielectric constant and substrate thickness. The measured insertion losses correspond well to the simulated ones.

Again, it can be seen that as N increases, second harmonic is shifted towards the higher frequencies. All structures successfully suppress a frequency band in the vicinity of the quasi-static resonance of the rings, positioned at approximately $2f_{c1}$. In that way, wide and deep stop bands in the transmission characteristics are created.

In Figure 8, LH lines using N=2 CSRRs and N=2 CSRs with optimized dimensions are compared. A good agreement between simulated and measured results can be observed, except for a shift in frequency approximately equal to 5%, explained as in the previous case. Also, measured insertion loss for the CSR case is somewhat lower then the simulated one.

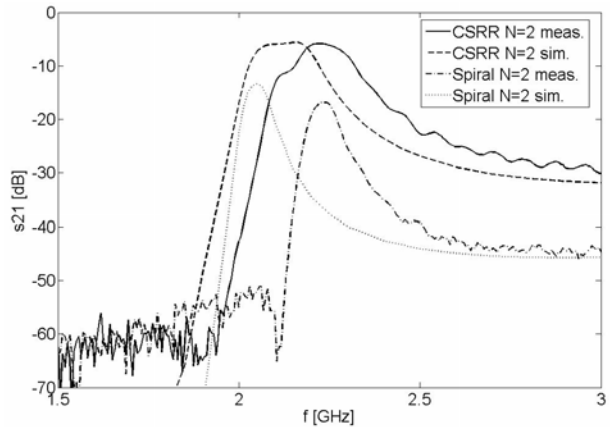

(a)

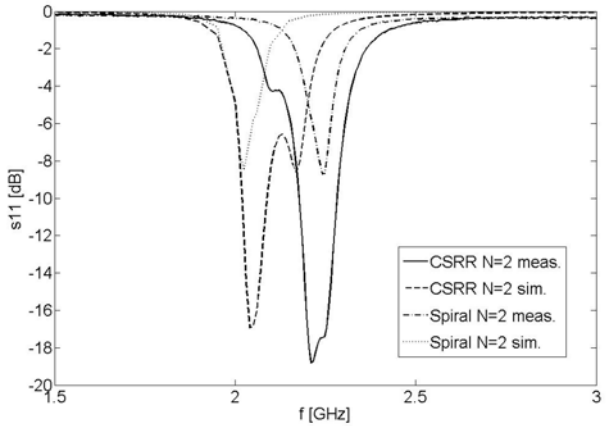

(b)

Figure 8 Simulation and measurement results for LH lines with *N*=2 CSRRs and *N*=2 CSRs with optimized dimensions: (a) transmission coefficient, (b) reflection coefficient

Results of the measurements performed in a wider frequency range, Figure 9, show that the application of CSRs results in a very wide and deep stop band, as well as in the higher frequency selectivity on both sides of the pass band then n the case of the CSRR, but also in much higher insertion loss.

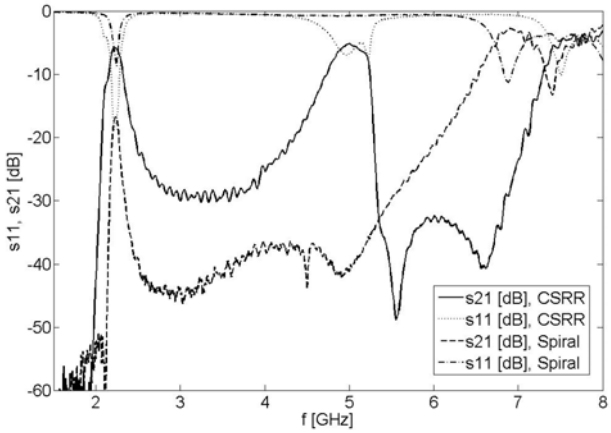

Figure 9 Measurement results for LH lines with *N*=2 CSRRs and *N*=2 CSRs with optimized dimensions, in a wider frequency range.

5. CONCLUSION

In this paper multiple split-ring and spiral geometries are investigated and compared. Influence of number of concentric rings and spiral turns, N, to the performances is analyzed. Two types of LH microstrip lines are designed and compared: the first using multiple CSRR geometries, and the second using multiple CSR geometries. It has been shown that as N increases, second harmonic was shifted towards the higher frequencies, thus creating wide and deep stop bands in the transmission characteristics. In the same time, the efficiency of excitation was reduced, thus resulting in weaker coupling of the particle to the host transmission line.

The dimensions of the CSR were optimized to achieve the same resonant frequency as the CSRR. It is shown that the application of CSR results in much compact solutions, with reduction of the particle's area for more then 66%, as well as in a wider and deeper stop band, and improved frequency selectivity on both sides of the pass band. However, this solution suffers from a high insertion loss, typical for all spiral geometries.

REFERENCES

[1] V. Veselago, "The electrodynamics of substances with simultaneously negative values of ε and μ," *Soviet Physics Uspekhi*, Vol. 92, no. 3, pp. 517-526, 1967.

[2] J. B. Pendry, A. J. Hoden, W. J. Stewart and I. Youngs, "Extremly low frequency plasmons in metallic mesostructures," *Physical Review Letters*, vol. 76, num. 25, pp. 4773-4776, 17 June 1996

[3] J. B. Pendry, A. J. Holden, D. J. Robbins and W. J. Stewart "Magnetism from conductors and enchanced nonlinear phenomena," *IEEE Transactions on microwave theory and technique*, vol. 47, no. 11, pp. 2075-2084, Novembar 1999.

[4] R. A. Shelby, D. R. Smith and S. Schultz: "Experimental verification of a negative index of refraction," Science, Vol. 292, pp. 77-79, 2001,

[5] R. Marqués, J. Martel, F. Mesa and F. Medina, "Left handed media simulation and transmission of EM waves in sub-wavelength SRR-loaded metallic waveguides", *Phys. Rev. Lett*., vol 89, pp. 183901-03, 2002.

[6] F. Martín, F. Falcone, J. Bonache, R. Marqués and M. Sorolla, "Miniaturized coplanar waveguide stop band filters based on multiple tuned split ring resonators", *IEEE Microwave Wireless Comp. Lett*., vol. 13, pp. 511-513, December 2003.

[7] F. Falcone, T. Lopetegi, M.A.G. Laso, J.D. Baena, J. Bonache, R. Marqués, F. Martín, M. Sorolla, "Babinet principle applied to the design of metasurfaces and metamaterials", *Phys. Rev. Lett.,* vol. 93, p 197401, November 2004.

LIST OF FIGURE CAPTIONS:

Figure 1 Microstrip line loaded with *N*=2 SRR

Figure 2 (a) SRR with *N*=2 (top) and *N*=9 (bottom) concentric rings, (b) SR with *N*=2 (top) and *N*=9 (bottom) turns

Figure 3 An example of the proposed LH microstrip line, using *N*=4 CSRRs

Figure 4 Transmission coefficient and phase propagation for the proposed LH microstrip lines with *M*=2 and *M*=3 unit cells

Figure 5 Comparison of the simulated responses of the proposed LH line using CSRs with different number of turns, *N*

Figure 6 Top (upper) and bottom (lower) sides of fabricated structures: LH line using (a) *N*=2 CSRRs, (b) *N*=3 CSRRs, (c) *N*=4 CSRRs, (d) *N*=2 CSRs with optimized dimensions.

Figure 7 (a) Simulation and (b) measurement results for LH lines using multiple CSRRs

Figure 8 Simulation and measurement results for LH lines with N=2 CSRRs and N=2 CSRs with optimized dimensions: (a) transmission coefficient, (b) reflection coefficient

Figure 9 Measurement results for LH lines with N=2 CSRRs and N=2 CSRs with optimized dimensions, in a wider frequency range.

LIST OF TABLE CAPTIONS:

TABLE 1 Simulation results for microstrip line loaded with SRR consisting of *N* concentric rings

TABLE 2 Simulation results for microstrip line loaded with SR consisting of N turns

TABLE 3 Simulation results for the proposed LH microstrip line using multiple CSRRs with *N* concentric rings

TABLE 4 Simulation results for the proposed LH microstrip line using multiple CSRs with N turns

TABLE 5 Simulation results for LH microstrip line using *N*=2 CSRRs and *N*=2 CSRs with optimized dimensions